Comparative Performance Analysis of Solar Tracking System Types at Different Latitudes

Mircea Neagoe and Bogdan Burduhos*

Renewable Energy Systems and Recycling R&D Centre, Transilvania University of Brasov, Brasov, Romania

Abstract: The increase of solar radiation collected by solar energy convertors is a major challenge in design process of photovoltaic or solar-thermal applications. A valuable approach refers to the use of solar tracking systems that support a large range of tracking performance according to their types, solar tracking algorithm or implementation location. The paper focuses on a comparative study, under the assumption of direct solar radiation only, of solar energy receiving share achieved by four tracking system types and various tracking algorithms used at different latitudes from the northern hemisphere. The simulation results showed a close connection of the tracking system type with the latitude, as well as high performance in collecting the solar energy of dual-axis and single-axis diurnal type tracking with optimized unequal steps.

Keywords: Direct solar radiation, Solar tracking, Tracking systems, Solar energy receiving share.

INTRODUCTION

Using local renewable energy resources, such as solar, wind, hydro and others for powering local consumers might be a solution for diminishing the conflict between energy-rich and energy-poor regions. Systems able to convert those renewable resources will represent important components that allow the generation of an energy mix with high sustainability share.

As solar radiation is the only resource available anywhere on the Earth's surface, the solar energy converters, *i.e*. photovoltaic (PV) modules and solar-thermal collectors, will play a key role in the transformation of the energy production sector [1, 2].

In order to use most of the available solar radiation, PV modules can be installed on solar tracking systems able to follow the Sun and to increase with up to 45% the yearly electricity production compared to optimally fix-tilted PV modules. The increase depends on the location latitude [3] and weather profile [4], but also on the number of the tracking system axes (single- or dual-axis) and implemented tracking algorithm [5, 6].

During intervals with clear sky, optimally fix-tilted solar converters collect only about 70% of the available solar energy. Depending on the weather profile, the yearly output gain of tracked converters can vary from ~20% in regions with unsteady weather to ~45% in regions with sunnier conditions. Further on, daily gain can vary even more, from ~0% during cloudy days to ~100% during clear sky days [7-9].

This output energy gain is especially important in areas with low solar radiation profile and in the built environment where installation space of PV modules is rather limited, but also comes with several disadvantages compared to fixed PV systems such as higher initial and operational costs [10-12].

Different types of tracking systems and tracking algorithms can be used for positioning solar converters towards the Sun, each of them with specific advantages and disadvantages.

The paper aims at identifying the optimal tracking system and algorithm that best fit different latitudes on the northern hemisphere. In order to achieve this goal, Section 2 of the paper describes the solar radiation which has two main components [13]: the direct radiation (B, maximal on the sunray's direction), and the diffuse radiation (D, maximal in the horizontal plane of the observer). Tracking applications are mainly suitable in locations with a solar radiation profile where B >> D [13]. Thus, the Section 2 also presents the modeling of four solar angle pairs and four tracking system types, which can be used for tracking the Sun.

Further, Section 3 describes solar tracking algorithms and the scenarios considered in numerical simulations. The numerical results are presented and discussed in Section 4, at several different latitudes from the northern hemisphere. The final conclusions are drawn in Section 5.

MODELLING APPROACH

The relative position of sunray vector on the Earth is defined by a pair of solar angles, which can be

*Address correspondence to this author at the Renewable Energy Systems and Recycling R&D Centre, Transilvania University of Brasov, Brasov, Romania; Tel: +40 268 413 000;
E-mail: bogdan.burduhos@unitbv.ro

E-ISSN: 2410-2199/21

expressed both in the global coordinate system of the Earth ($OX_0Y_0Z_0$) and in the local observer coordinate system (QXYZ), where the Q site is located at a latitude φ (Figure **1**). The point O is the Earth's centre, Z_0 is the South-North rotation axis of the Earth and Y_0 is given by the intersection of the local meridian and the equatorial plane. The axis Z corresponds to the local vertical (zenith) axis, Y to the north direction and X to the East direction.

The solar angles in the global coordinate system, *i.e.* equatorial type solar angles, are (Figure **1a**):

- *declination angle* δ, stated as the angle between the sunray and the equatorial plane;
- *hour angle* ω, the angle between the sunray projection line in the equatorial plane and $-Y_0$ axis.

The angle δ ranges during the year between -23.45° and +23.45°, as the Earth axis is tilted 23º26'21" from the normal vector of its orbit plane; its average daily variation is about 0.25° and hence in practice the δ angle is considered constant over one day:

$$\delta = 23.45^\circ \sin\left(\frac{2\pi(\mathrm{N}-80)}{365}\right) \tag{1}$$

where *N* is the day number of the year.

The hour angle of the Sun changes with 15°/hour and it can be calculated using:

$$\omega = 15^\circ\left(12 - \mathrm{t_s}\right) \tag{2}$$

where t_s is the solar time.

The sunray vector can be also projected on the three orthogonal planes of the local coordinate system QXYZ, and the following solar angle pairs result [1, 14]:

- (ψ, α): azimuth type solar angles, where the sunray vector is projected on the horizontal plane, Figure **1b**;
- (ε, ρ): pseudo-azimuth type solar angles, obtained by projecting the sunray vector on the vertical W-E plane, Figure **1c**;
- (β, γ): pseudo-equatorial type solar angles, if the sunray vector is projected on the vertical N-S plane, Figure **1d**.

The solar angles ψ (also named azimuth), ε and β are diurnal angles and describe the Sun relative motion from East (sunrise) toward West (sunset). The elevation of the Sun on the sky is modelled by the solar elevation angles α (denoted also as altitude angle), ρ and γ, respectively.

Assuming that the sunrays are parallel, the solar angle pairs can be computed in relation to the equatorial type solar angles as follows [1]:

$$\begin{cases}\alpha = asin(cos\omega cos\delta cos\varphi + sin\delta sin\varphi)\\ \psi = 2atan\left(\frac{sin\omega cos\delta}{cos\alpha + cos\omega cos\delta sin\varphi - sin\delta cos\varphi}\right)\end{cases} \tag{3}$$

$$\begin{cases}\rho = asin(cos\omega cos\delta sin\varphi - sin\delta cos\varphi)\\ \varepsilon = 2atan\left(\frac{sin\omega cos\delta}{cos\rho + cos\omega cos\delta cos\varphi + sin\delta sin\varphi}\right)\end{cases} \tag{4}$$

$$\begin{cases}\gamma = atan\left(\frac{cos\omega cos\delta sin\varphi - sin\delta cos\varphi}{cos\omega cos\delta cos\varphi + sin\delta sin\varphi}\right)\\ \beta = 2atan\left(\frac{sin\omega cos\delta cos\gamma}{cos\gamma + cos\omega cos\delta cos\varphi + sin\delta sin\varphi}\right)\end{cases} \tag{5}$$

Based on these four solar angle pairs, four types of tracking systems can be developed, Figure **2**:

- *Equatorial* (or *polar*) type (further denoted by *Eq*) – Figure **2a**, where the diurnal axis is parallel to the Earth polar axis [15-17];
- *Azimuth (*or *azimuth-altitude)* type (*Az*) – Figure **2b**, where the diurnal axis is parallel to the zenith (local vertical axis) [16-20];
- *Pseudo-Equatorial* type (*PEq*) – Figure **2c**, where the fixed horizontal rotation axis is parallel to the E-W direction [3, 14, 20, 21];
- *Pseudo-Azimuth* type (*PAz*) – Figure **2d**, with a fixed horizontal rotation axis parallel to N-S direction [3, 14, 20, 21].

The dual-axis tracking systems contain two revolute joints with reciprocating perpendicular axes, where the first (primary) axis is fixed relative to the ground, and the second (secondary) axis is perpendicular to the first axis. The primary axis is used for daytime movement, and the secondary axis for the elevation movement, except the pseudo-equatorial system (*PEq*), where the role of the two motion axes is reversed.

The amount of solar energy collected by a tracked receiving surface depends on the available solar radiation and on the tracking program that controls the daily motion of the tracking mechanism typically aiming at increasing the received irradiance of the direct solar radiation. The available and collected direct solar radiation can be modelled using the Meliss approach [22], as follows.

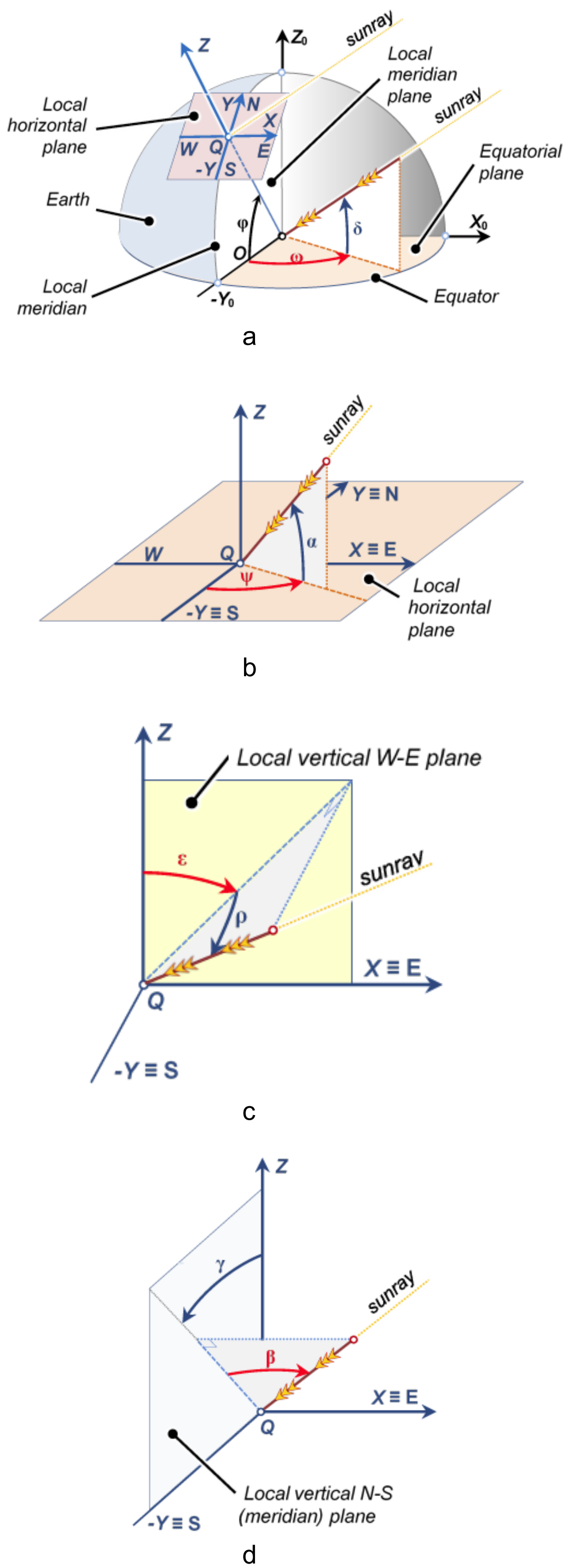

Figure 1: Solar angle pairs of type: **a**. Equatorial; **b**. Azimuth; **c**. Pseudo-Azimuth; **d**. Pseudo-Equatorial.

The extra-terrestrial solar irradiance B_0, measured in a plane orthogonal to the sunray, is considered constant during a day N, close to the solar constant I_0 = 1361.1W/m^2 [23]:

$$B_0 = I_0 \left[1 + 0.0334 \cos\left(\frac{\pi}{180}(0.9856N - 2.72) \right) \right]. \tag{6}$$

The irradiance B [W/m^2] of direct solar radiation available at the ground surface (measured in a plane orthogonal to the sunray) is a time-dependent parameter also depending on the path length and the composition of the Earth atmosphere layers passed by the sunray in clear sky conditions:

$$B = B_0 e - \frac{T_R}{0.9 + 9.4\ sin\alpha,} \tag{7}$$

where T_R represents the direct radiation loss (Linke) factor.

The irradiance B_n [W/m^2] of the direct solar radiation collected by a planar receiving surface with the normal unit vector can be derived from the Lambert law:

$$B_n = B \cos \nu, \tag{8}$$

where the incidence angle ν of the sunray on surface can be set in the equatorial (Eq), azimuth (Az), pseudo-azimuth (PAz) and pseudo-equatorial (PEq) reference system, respectively, by using [1]:

$$\cos \nu = \tag{9}$$

$$cos\delta cos\delta_n cos(\omega - \omega_n) + sin\delta\ sin\delta_n =$$
$$cos\alpha cos\alpha_n cos(\psi - \psi_n) + sin\alpha\ sin\alpha_n =$$
$$cos\rho cos\rho_n cos(\varepsilon - \varepsilon_n) + sin\rho\ sin\rho_n =$$
$$cos\beta cos\beta_n cos(\gamma - \gamma_n) + sin\beta\ sin\beta_n.$$

The main criterion used in the comparative analysis within this study is the average receiving share of the direct solar radiation (η_B):

$$\eta_B = \frac{E(B_n)}{E(B)} = \frac{\int B_n dt_s}{\int B dt_s}. \tag{10}$$

where E(Bn) and E(B) are the energy over one day/month/year of the received and available direct solar radiation, respectively.

SOLAR TRACKING ALGORITHMS AND SIMULATION SCENARIOS

The tracking algorithms are designed to optimize (generally to maximize) the solar energy collection by

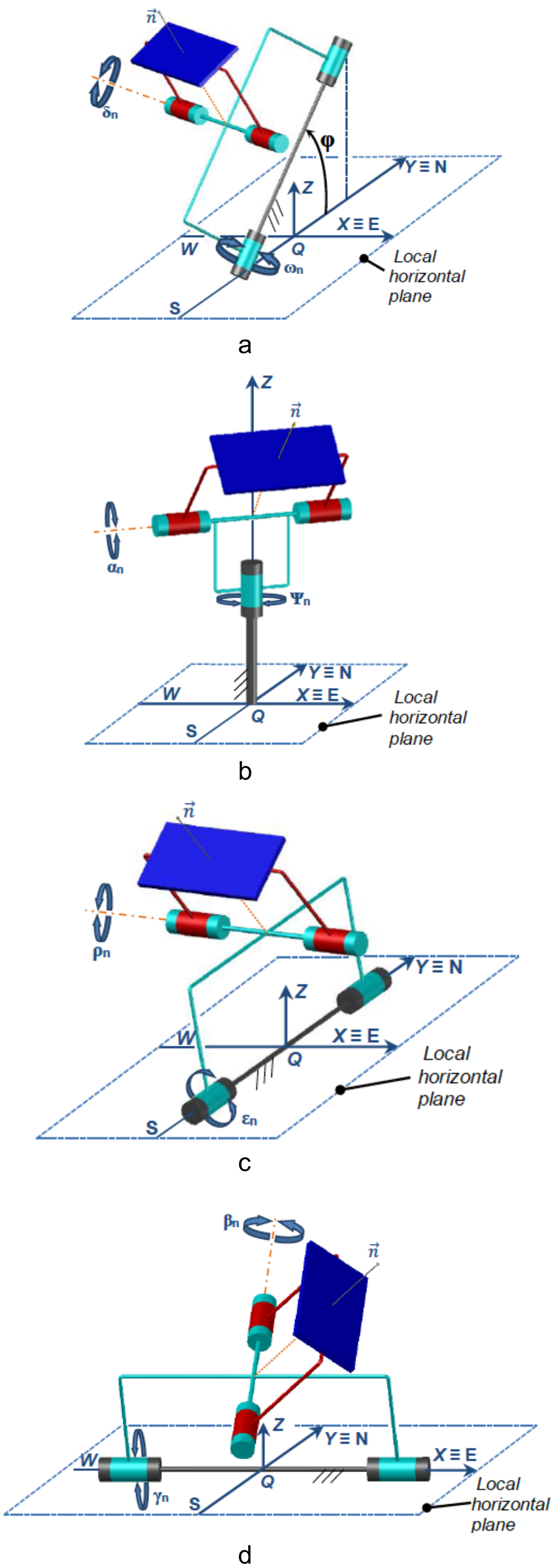

Figure 2: Dual-axis tracking system types: **a**. Equatorial; **b**. Azimuth; **c**. Pseudo-Azimuth; **d**. Pseudo-Equatorial.

tracking the Sun's position on the sky. The steps of the tracking algorithm are implemented into a tracking program that controls the angular displacements on the tracking mechanism axes. The tracking programs commonly used in practice are stepwise: the mechanical system is kept at rest during the most of the time, followed by a rather short period of operation (several seconds) to bring the solar converter's surface into a new optimal position. A tracking program represents a sequence of commands (u, t), whereby the movement from the current angular position to the new position *u* is triggered at the time *t*.

This comparative study on the received solar energy share considered all the four types of tracking systems (Az, Eq, PAz, PEq), using different tracking programs (continuous and stepwise) and different tracking scenarios (single-axis, dual-axis) by focusing only the effect of the direct solar radiation, *i.e*. neglecting de diffuse and reflected (Albedo) solar radiation. This numerical simulations are developed for sites located at different latitudes in the northern hemisphere (Equator 0°, 15°N, 30°N, 45°N and 60°N), on the meridian 25.5°E (Figure **3**). The Linke factor T_R, required to calculate the solar irradiance B according to Eq. (7), was obtained for each location from the SoDa database [24].

Continuous tracking has a strictly theoretical value, identifying the performance limit of a tracking system, while in practice stepwise tracking is used. Beyond to the classic tracking method with equal steps on large angular strokes, tracking with unequal optimized steps allows high receiving share of solar radiation, close to those of continuous tracking but with lower angular strokes [1, 12].

Figure 3: Case study sites located at different latitudes on the 25.5°E meridian.

For a mid-latitude location (45°N, Figure **4**) and considering the optimal monthly adjustment of the tilt angle, the solar energy receiving share by using diurnal tracking with two unequal steps is over 90% regardless of the month (Figure **4a**) and over 94% in the case of annual average values, regardless of the tracking system type (Figure **4b**).

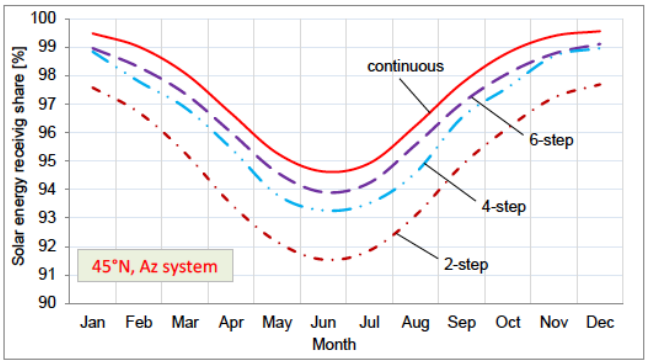

a

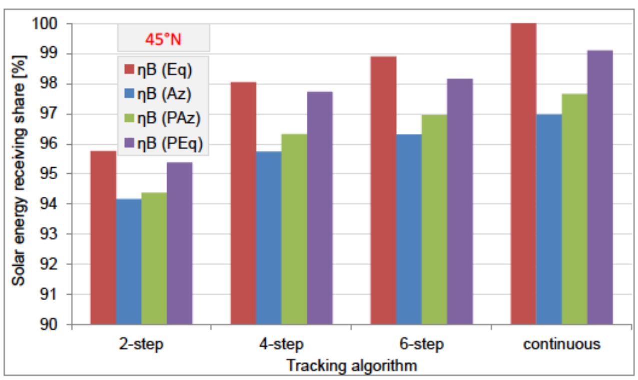

b

Figure 4: Solar energy receiving efficiency using diurnal stepwise (2-, 4- and 6-step) vs. continuous tracking algorithm with monthly optimal tilt angle at 45°N latitude: **a**. monthly variation in case of azimuth-type tracking; **b**. yearly average values for all four tracking types.

The performance difference between continuous and 6-step tracking is less than 1%, followed closely by the 4-step tracking (less than 1.5%). Therefore, 4-step tracking was selected for the following comparative analysis as a representative tracking algorithm with unequal steps.

The following tracking scenarios have been analysed and compared with fixed South-oriented systems tilted at the latitude angle (*Scenario 0*, further denoted by *S0*):

1. *Scenario 1 (S1)*: fixed diurnal angle set at 0° and optimal elevation angle, monthly adjusted;
2. *Scenario 2 (S2)*: fixed diurnal angle set at 0° and stepwise elevation tracking program with four unequal optimised steps;
3. *Scenario 3 (S3)*: stepwise diurnal tracking program with four unequal optimised steps and fixed tilt angle set at latitude value;
4. *Scenario 4 (S4)*: stepwise diurnal tracking program with four unequal optimised steps and optimal elevation angle, monthly adjusted;
5. *Scenario 5 (S5)*: stepwise diurnal and elevation tracking programs with four unequal optimised steps.

The role of single-axis tracking of elevation type in collecting direct solar radiation during various seasons is investigated through the Scenarios 1 and 2. The benefit of single-axis tracking of diurnal type is identified through the Scenario 3. Moreover, dual-axis tracking is also considered for investigating the impact stepwise programs in collecting solar radiation (Scenarios 4 and 5).

RESULTS AND DISCUSSION

Based on the analytical model described by relations (1)… (10), the solar energy receiving share is simulated (as monthly and annual average value) for each of the five selected locations (Figure **3**), considering the scenarios S0… S5 and each of the four types of tracking systems (Eq, Az, PAz, PEq). The monthly results address only the mid-latitude of 45°N, as a relevant example, but the annual results are presented for all selected latitudes.

The average receiving share of the direct solar radiation (η_B) at the latitude 45°N, Figure **5** and Figure **6**, allow to formulate the following remarks:

- By monthly adjusting the optimal tilt angle (Scenario S1), a South-facing surface can collect an average monthly share of direct solar energy ranging between 67% (in June) and 88% (in December), and 73% during the year. A South-facing surface permanently fixed and tilted at 45° can collect yearly approximately 68% of the available solar direct radiation, B. As a results, the solar energy yearly gain by using the Scenario S1 is about 5% compared with the Scenario S0, with the higher value of about 12% in June (Figure **6**).

- Single-axis, 4-step elevation tracking with fixed diurnal angle set at 0° (Scenario S2) does not bring a significant gain to the collected solar radiation compared to the Scenario S1, Figure **5**. Moreover, the tracking systems of PAz and Eq type generally lead to a slightly decreasing of the receiving share, an increased share using an PEq type system (Figure **6d**), and to a significant loss in case of Az type system (Figure **6b**), even compared to the Scenario 0. As result, the stepwise elevation tracking can be replaced by adjusting the elevation angle to the optimal monthly or even to the annual value in case of the Az type system (Figure **5d**).

- Oppositely, the single-axis 4-step diurnal tracking with fixed elevation angle set at latitude value (Scenario 3) supports the yearly collection of min. 87% of the available direct solar radiation, regardless the tracking system type (Figure **5d**). The results also show that there is a higher performance when using the Eq and PEq tracking systems, while lower yearly performances are recorded for the PAz tracking system (Figure **5d**). During the summer months, the best performances are achieved by the Az type system (Figure **6b**), while the worst case is registered by the PAz type tracking (Figure **6c**).

- The Scenario 4 (4-step diurnal tracking with adjusting monthly the optimal fixed elevation angle) allow increasing the monthly average receiving share over 93%, regardless the month and tracking system type (Figure **5a**…**c**). The receiving share records yearly average values over 96% (Figure **5d**). The lower values of the solar energy-receiving share are registered during the summer month by the Az type system (Figure **6b**, 93%) and PAz type system (Figure **6c**, 95%).

- The receiving share values in the Scenario 5 (dual-axis 4-step tracking) ranges between 97% (June) and 99% (December), and 98% yearly average value. All four types of tracking systems are able to rich the same optimal positions of the receiving surface and thus the same solar energy-receiving share in any month, with a slight variation over the year (Figure **6**).

The annual average values of the receiving share vary significantly with the latitude, as shown in Figure **7** and Figure **8**; accordingly, the following aspects can be highlighted:

- The receiving share of the direct solar radiation decreases by down to 8% from the Equator to the 60°N latitude for fix-tilted receiving surfaces (Scenario S0) and single-axis elevation tracking with monthly adjustment of the tilt angle (Scenario S1), Figure **7** and Figure **8a**. In the fix-tilted approach the receiving share falls below

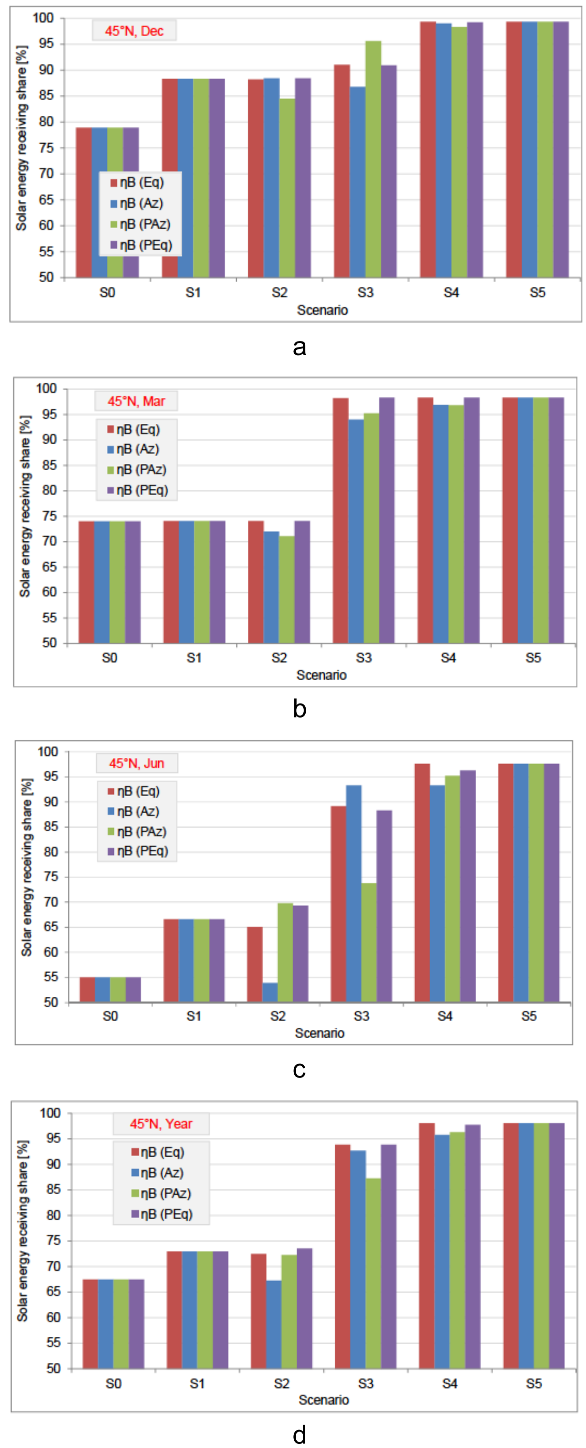

Figure 5: Average energy receiving share of direct solar radiation at mid-latitude 45°N using the strategies S0…S5 during: **a**. December; **b**. March; **c**. June; **d**. Year.

65% (S0) and 75% (S1) at higher latitudes, where solar tracking becomes an attractive option. Thus, dual-axis 4-step tracking (S5, Figure **7** and Figure **8a**) maintains high receiving share (over 98%) at all latitudes and brings a significant gain at high latitudes of over 50% compared to the fix-tilted Scenario 0.

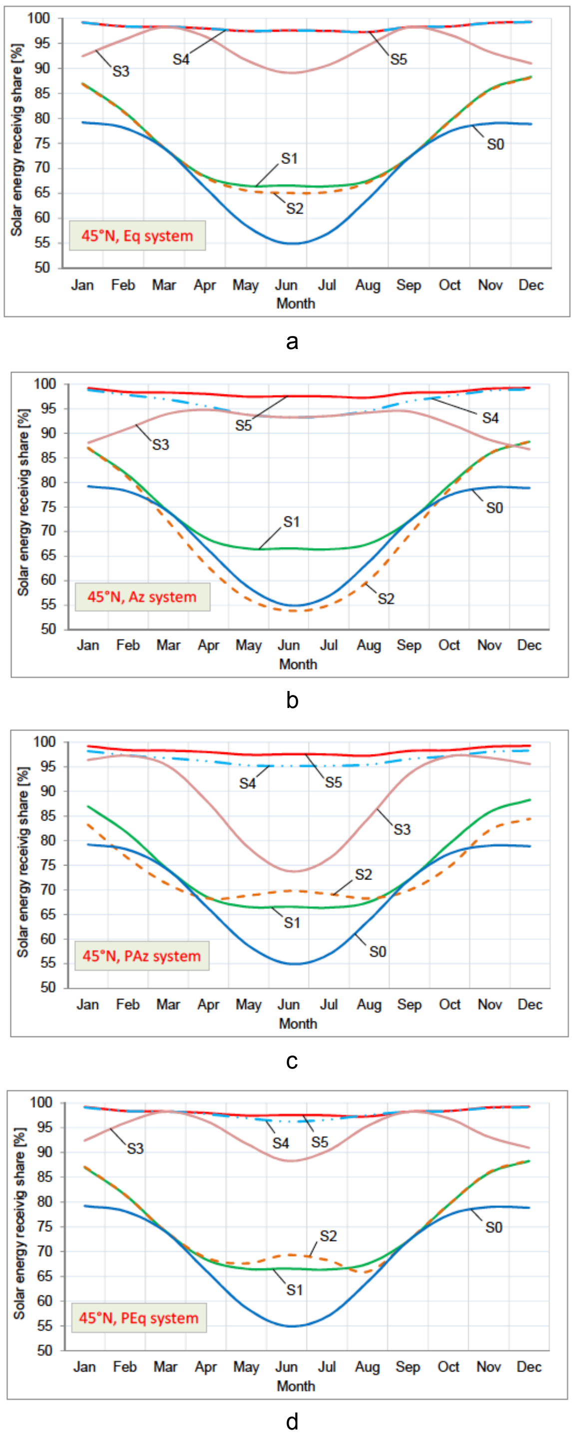

Figure 6: Monthly variation of the average receiving share of direct solar radiation collected by a tracking system of: **a**. equatorial Eq type; **b**. azimuth Az type; **c**. pseudo-azimuth PAz type; **d**. pseudo-equatorial PEq type.

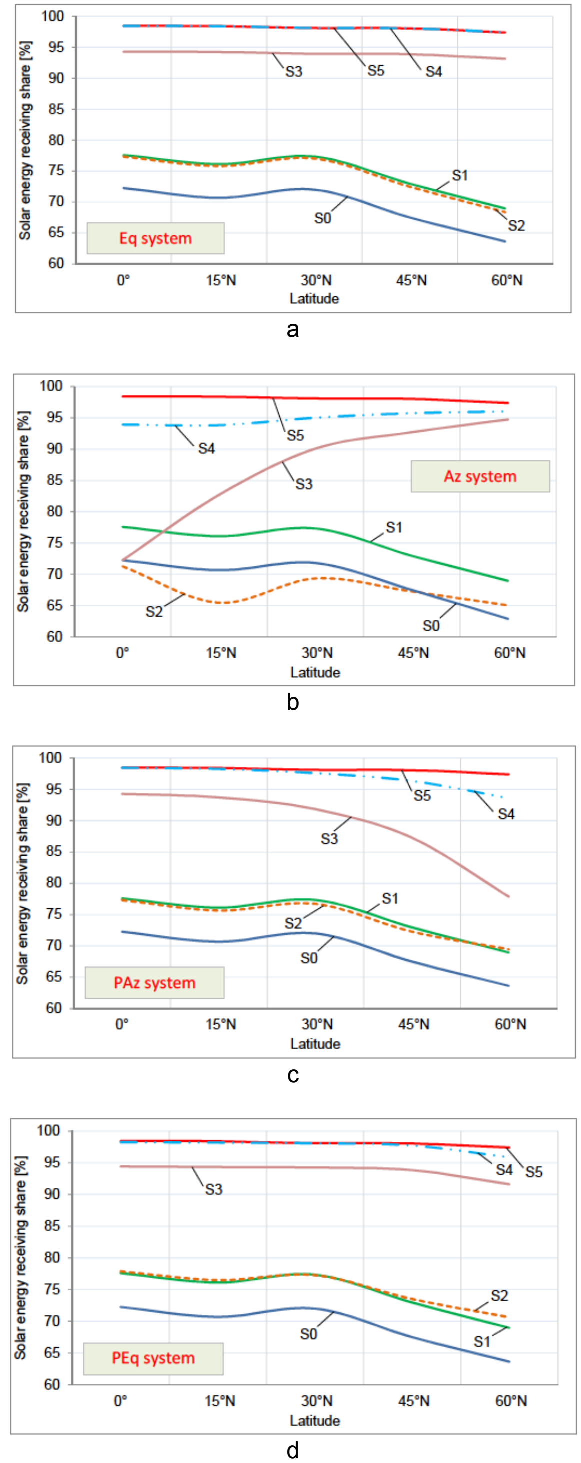

Figure 7: Variation over latitudes of the average receiving share of direct solar radiation collected yearly by a tracking system of: **a**. Equatorial Eq type; **b**. Azimuth Az type; **c**. Pseudo-azimuth PAz type; **d**. Pseudo-equatorial PEq type.

- The Scenario 2 (4-step elevation tracking, Figure **7** and Figure **8b**) is not recommended for practical applications, irrespective of latitude, as its solar energy receiving performance is generally similar to the simpler Scenario 1 in

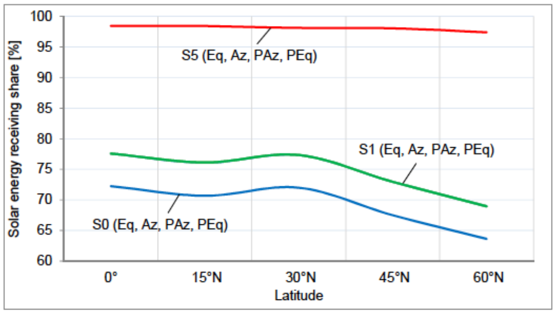

a

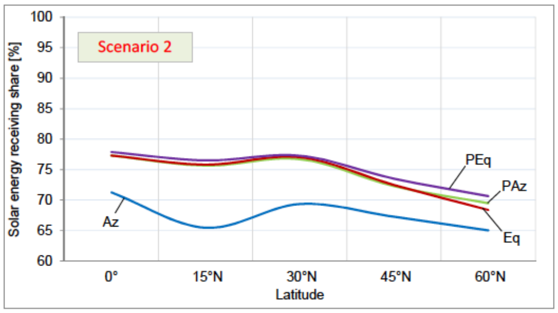

b

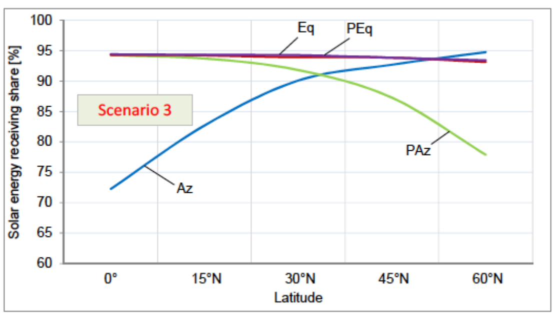

c

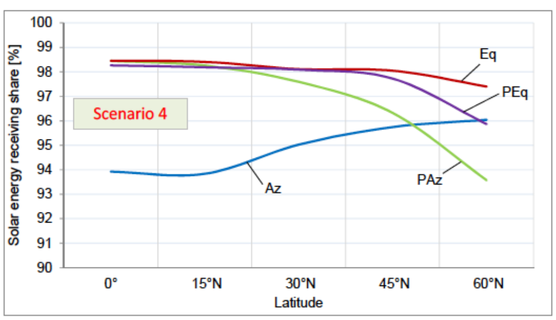

d

Figure 8: Variation over latitudes of the average receiving share of direct solar radiation collected yearly by using four tracking system types (Eq, Az, PAz, PEq) for: **a**. Scenarios S0, S1 and S5; **b**. Scenario 2; **c**. Scenario 3; **d**. Scenario 4.

case of Eq, PAz and PEq tracking systems. Moreover, the Az tracking use leads to a significant decrease of the receiving share with worse behaviour even than Scenario 0.

- Single-axis stepwise diurnal tracking (Scenario 3, Figure **7** and Figure **8c**) proves to have superior performance compared to single-axis elevation tracking (Scenario 2). In this scenario, the Eq and PEq tracking systems have identical performance and ensure receiving shares of about 94-95% at all latitudes. In contrast, the PAz diurnal tracking system has superior performance only at low latitudes, while the Az system best performs only at high latitudes.

- In Scenario 4 (Figure **7** and Figure **8d**), obtained by extending the Scenario 3 with monthly adjustment of the tilt angle, a significant improvement of the receiving share is obtained compared to Scenario 3, closed to the Scenario 5. Thus, the Eq and PEq systems achieve values of receiving share of over 98% at low latitudes and over 96% at high latitudes. The PAz system best performs at low latitudes and decreases rapidly the receiving share at latitudes higher than 30° (down to 93-94%). Contrary, the Az system increases the receiving share with the latitude increase, but without exceeding 96%.

Therefore, the implementation location represents a key factor in selecting an optimal solar tracking solution, considering the tracking system type and the tracking algorithm.

CONCLUSIONS

The paper presents an overview on the solar energy receiving performance of four types of tracking systems, analysed over one year at different latitudes for various tracking algorithms, in the assumption of considering only direct solar radiation, as solar tracking is valuable mainly on sunnier locations, during sunny days or clear sky time periods.

The obtained simulation results allow drawing the following final conclusions:

- The stepwise tracking is an efficient approach of increasing of the solar energy receiving share over the year, irrespective of latitude. Dual-axis 4-step tracking enables receiving share up to 98%, single-axis diurnal tracking supports receiving share up to 94-95%, while optimal fix-tilted approach allows collecting about 64-72% of the available solar energy.

- Single-axis elevation tracking has significantly lower performance compared to single-axis diurnal tracking, as it allows receiving shares of about 69-78%.

- Compared to the optimal fix-tilted systems, the solar energy collected by diurnal tracking is higher (almost double) during the summer months and significant (up to 50%) in the transient seasons (spring, autumn). Oppositely, only slight gains are recorded in winter, leading to the idea of implementing a fixed and tilted at optimal angle value for this season.

- For single-axis diurnal tracking, the Equatorial Eq and Pseudo-equatorial PEq systems perform better irrespective of the latitude. The Azimuth Az type systems are recommended only at high latitude, while the Pseudo-azimuth PAz systems at low latitudes. Dual-axis tracking systems ensures identical receiving share regardless their types.

These results can be extended to locations on other meridians, as well as for the southern hemisphere.

The selection of a solar tracking system is a complex procedure, where the solar energy receiving share is one of the critical criteria. Other criteria can be added, such as the tracking angles strokes or the complexity of the tracking system.

NOMENCLATURE

α	= altitude solar angle
α_n	= altitude tracking angle
β	= diurnal solar angle of pseudo-equatorial type
β_n	= diurnal tracking angle of pseudo-equatorial type
γ	= elevation solar angle of pseudo-equatorial type
γ_n	= elevation tracking angle of pseudo-equatorial type
δ	= declination solar angle
δ_n	= declination tracking angle
ε	= diurnal solar angle of pseudo-azimuth type
ε_n	= diurnal tracking angle of pseudo-azimuth type
η_B	= average receiving share of the direct solar radiation
v	= incidence angle
ρ	= elevation solar angle of pseudo-azimuth type
ρ_n	= elevation tracking angle of pseudo-azimuth type
φ	= latitude angle
ψ	= azimuth solar angle
ψ_n	= azimuth tracking angle
ω	= hour solar angle
ω_n	= hour tracking angle
Az	= azimuth type
B_0	= extra-terrestrial solar irradiance
B	= irradiance of available direct solar radiation at ground level
B_n	= received direct solar radiation
D	= irradiance of available diffuse solar radiation at ground level
Eq	= equatorial type
E(B)	= energy of the available direct solar radiation
E(Bn)	= energy of the received direct solar radiation
I_0	= solar constant
N	= day number of the year
$\vec{n}$	= normal unit vector of the receiving surface
PAz	= pseudo-azimuth type
PEq	= pseudo-equatorial type
PV	= photovoltaic
T_R	= direct radiation loss (Linke) factor
t_s	= solar time

REFERENCES

[1] Visa I, Duta A, Moldovan M, Burduhos BG, Neagoe M. Solar energy conversion systems in the built environment. Springer, Cham, Switzerland; 2020. https://doi.org/10.1007/978-3-030-34829-8

[2] Burduhos BG, Visa I, Neagoe M, Devetakovic M, Cretescu NR. Comparative Analysis of Software Accuracy in Photovoltaic Energy Estimation for a Temperate Mountain Climate. In: Visa I, Duta A, editors. Solar Energy Conversion in Communities. Springer Proceedings in Energy. Springer, Cham 2020; 125-139. https://doi.org/10.1007/978-3-030-55757-7_9

[3] Burduhos BG, Toma C, Neagoe M, Moldovan MD. Pseudo-Equatorial Tracking Optimization for Small Photovoltaic Platforms from Toronto/Canada. Environmental Engineering and Management Journal 2011; 10(8): 1059-1068. https://doi.org/10.30638/eemj.2011.154

[4] Burduhos BG, Visa I, Duta A, Neagoe M. Analysis of the conversion efficiency of five types of photovoltaic modules during high relative humidity time periods. Journal of Photovoltaics 2018; 8(6): 1716-1724. https://doi.org/10.1109/JPHOTOV.2018.2861720

[5] Visa I, Diaconescu D, Popa V, Burduhos BG, Saulescu R. The synthesis of a linkage with linear actuator for solar

tracking with large angular stroke. Proceedings of EUCOMES 08. 2008; 447-454. https://doi.org/10.1007/978-1-4020-8915-2_54

[6] Quaglia G, Maurino SL. Solar.q_1: A new solar-tracking mechanism based on four-bar linkages. Proc. IMechE Part C: J Mechanical Engineering Science 2016; 231(15): 2855-2867. https://doi.org/10.1177/0954406216641454

[7] Tracstar. Small Power Systems Has Built Trackers for Over 25 Years. Available from:http://www.helmholz.us/smallpowersystems/. Accessed 2020/12/04.

[8] Abdallah S. The effect of using sun tracking systems on the voltage-current characteristics and power generation of flat plate photovoltaics. Energ Convers Manage 2004; 45: 1671-1679. https://doi.org/10.1016/j.enconman.2003.10.006

[9] Sungur C. Sun-Tracking System with PLC Control for Photo-Voltaic Panels. International Journal of Green Energy 2007; 4(6): 635-643. https://doi.org/10.1080/15435070701665404

[10] Paris E, Beisner K. Fixed-Tilt vs. Tracker: Why a One-Size-Fits-All Approach Can Limit Solar Production. SPW, 2018.

[11] Greentech Media. Solar Balance-of-System: To Track or Not to Track, Part I. 2012. Available from: https://www.greentechmedia.com/articles/read/solar-balance-of-system-to-track-or-not-to-track-part-I. Accessed 2020/12/04.

[12] Neagoe M, Burduhos BG, Mohammadi F, Cretescu NR. A Comparative Analysis of the Solar Energy Receiving Share Using Four Tracking System Types at Mid-Latitude Regions. In: Visa I, Duta A, editors. Solar Energy Conversion in Communities. Springer Proceedings in Energy. Springer, Cham; 2020. https://doi.org/10.1007/978-3-030-55757-7_7

[13] Burduhos BG, Visa I, Neagoe M, Badea M. Modeling and optimization of the global solar irradiance collecting efficiency. International Journal of Green Energy 2015; 12(7): 743-755. https://doi.org/10.1080/15435075.2014.884499

[14] Visa I, Jaliu C, Duta A, Neagoe M, Comsit M, Moldovan M, Ciobanu D, Burduhos B, Saulescu R. The role of mechanisms in sustainable energy systems. Transilvania University Pub. House, Brasov; 2015.

[15] Davies PA. Sun-tracking mechanism using equatorial and ecliptic axes. Sol Energy 1993; 50(6): 487-489. https://doi.org/10.1016/0038-092X(93)90110-A

[16] Lee CY, Chou PC, Chiang CM, Lin CF. Sun Tracking Systems: A Review. Sensors-Basel 2009; 9: 3875-3890. https://doi.org/10.3390/s90503875

[17] Nsengiyumva W, Chen SG, Hu L, Chen X. Recent advancements and challenges in Solar Tracking Systems (STS): A review. Renew Sust Energ Rev 2018; 81: 250-279. https://doi.org/10.1016/j.rser.2017.06.085

[18] Koussaa M, Haddadib M, Saheba D, Maleka A, Hadjic S. Sun tracking mechanism effects on flat plate photovoltaic system performances for different step time and main parameters affecting the obtained gains: case of North Africa and Mediterranean site. Energy Procedia 2012; 18: 817-838. https://doi.org/10.1016/j.egypro.2012.05.097

[19] Miloudi L, Acheli D, Chaib A. Solar Tracking with Photovoltaic Panel. Energy Procedia 2013; 42: 103. https://doi.org/10.1016/j.egypro.2013.11.010

[20] Visa I. Renewable energy systems: case study - solar energy conversion systems. In: Visa I, editor. Mechanisms and Machine Science, Springer, Cham 2014; 18:31. https://doi.org/10.1007/978-3-319-01845-4_4

[21] Diaconescu DV, Vatasescu M. Two new pairs of local solar angles and their corresponding tracking systems. Bulletin of the Transilvania University of Brasov 2008; 1(50): 113-120.

[22] Meliss M. Regenerative Energiequellen - Praktikum. Springer, Heidelberg; 1997. https://doi.org/10.1007/978-3-642-60864-3

[23] Gueymard C.A. A reevaluation of the solar constant based on a 42-year total solar irradiance time series and a reconciliation of spaceborne observations. Solar Energy 2018; 168: 2-9. https://doi.org/10.1016/j.solener.2018.04.001

[24] SoDa. Solar radiation Data. Available from: www.soda-pro.com. Accessed 2020/11/10.

Received on 28-12-2020 Accepted on 19-2-2021 Published on 18-3-2021

DOI: https://doi.org/10.31875/2410-2199.2021.08.1